Computer simulation study of a simple tetrahedratic mesogenic lattice model

Silvano Romano*

Unità di Ricerca CNISM e Dipartimento di Fisica "A. Volta," Università di Pavia, via A. Bassi 6, I-27100 Pavia, Italy

(Received 23 July 2007; revised manuscript received 6 November 2007; published 8 February 2008)

Over the last 12 years, the possible existence of a tetrahedratic mesophase, involving a third-rank orientational order parameter and no positional order, has been addressed theoretically and predicted in some cases; no experimental realizations of a purely tetrahedratic phase are known at the time being, but various pieces of evidence suggest that interactions of tetrahedral symmetry do play a significant role in the macroscopic properties of mesophases resulting from banana-shaped (bent-core) mesogens. We address a very simple tetrahedratic mesogenic lattice model, involving continuous interactions; we consider particles possessing T_d symmetry, whose centers of mass are associated with a three-dimensional simple-cubic lattice; the pair potential is taken to be isotropic in orientation space and restricted to nearest-neighboring sites; we let the two orthonormal triads $\{\mathbf{u}_\alpha,\ \alpha=1,2,3\}$ and $\{\mathbf{v}_\gamma,\ \gamma=1,2,3\}$ define the orientations of a pair of interacting particles; we let the unit vectors $\mathbf{u}_\alpha$ be combined to yield four unit vectors $\{\mathbf{e}_j,\ j=1,2,3,4\}$, arranged in a tetrahedral fashion; we let the unit vectors $\mathbf{v}_\gamma$ be similarly combined to yield the four unit vectors $\{\mathbf{f}_k,\ k=1,2,3,4\}$; and finally we let $h_{jk}=(\mathbf{e}_j\cdot\mathbf{f}_k)$. The interaction model studied here is defined by the simplest nontrivial (cubic) polynomial in the scalar products h_{jk}, consistent with the assumed symmetry and favoring orientational order; it is, so to speak, the tetrahedratic counterpart of the Lebwohl-Lasher model for uniaxial nematics. The model was investigated by molecular field (MF) theory and Monte Carlo simulations; MF theory predicts a low-temperature, tetrahedrically ordered phase, undergoing a second-order transition to the isotropic phase at higher temperature; on the other hand, available theoretical treatments point to the transition being driven first order by thermal fluctuations. Simulations showed evidence of a first-order transition.

DOI: 10.1103/PhysRevE.77.021704 PACS number(s): 61.30.−v, 61.30.Cz, 61.30.Gd, 64.70.M−

I. INTRODUCTION AND POTENTIAL MODELS

Nematic liquid crystals are usually apolar and uniaxial, although their constituent molecules do not possess such high symmetries; on the other hand, over the last few decades, a number of theoretical investigations have addressed the possibility of orientationally ordered phases with different symmetries and no positional order; in turn, these theoretical results have prompted various attempts to produce experimental realizations, and the task has often proven to be rather difficult.

For example, since 1970, various theoretical treatments had predicted the possible existence of biaxial nematic phases; stable biaxial phases had been observed in lyotropic systems as early as 1980; in the following years there had been some claims and counterclaims of synthesizing and unambiguously characterizing a thermotropic biaxial nematic, and better experimental evidence seems to have been produced over the last two years (see, e.g., Refs. [1–4]); a more extensive discussion and a detailed bibliography can be found in Refs. [5,6].

Another example, where no experimental realization is known to date, involves the possible existence of a cubatic mesophase, possessing cubic orientational order (i.e., along three mutually orthogonal axes); this has been investigated theoretically [7] and explicitly predicted in some specific cases, involving both hard-core [8] and continuous interaction models [9]. A more extensive discussion and a detailed bibliography can be found, e.g., in Ref. [9].

The possibility of tetrahedratic orientational order, involving a third-rank order parameter was proposed and studied by Fel [10,11]; its transitional behavior was later studied by Radzihovsky and Lubensky [12,13], and the macroscopic consequences of tetrahedratic order were discussed in detail by Cladis, Brand, and Pleiner [14–16]; a detailed symmetry classification of "unconventional" nematic phases—i.e., associated with the onset of either one tensor of rank different from 2 or of several combined tensors—has recently been carried out by Mettout [17].

Also starting in the mid-1990s, bent-core (banana-shaped) mesogen were synthesized [18] and found to produce mostly smectic, and sometimes also nematic [19], phases; in some cases, evidence of thermotropic biaxial nematic behavior has been found in them [1–4]; numerical simulation studies have been undertaken as well (see, e.g., Refs. [20,21]). No experimental realizations of a purely tetrahedratic phase are known at the time being, and no third-rank order parameter has been measured to date, but the theoretical analyses in Refs. [12–16] show that interactions of tetrahedral symmetry (or, in more general terms, a description allowing for first-, second-, and third-rank ordering tensors) are needed for the proper comprehension of macroscopic properties of mesophases resulting from bent-core molecules.

On the other hand, over the decades, mesophases possessing no positional order, such as the nematic one, have often and quite fruitfully been studied by means of lattice models involving continuous interaction potentials [22,23], starting with the model proposed by Lebwohl and Lasher (LL) and used for their seminal simulation papers in the early 1970s [24,25]; this approach also yields a convenient contact with molecular field (MF) treatments of the Maier-Saupe (MS) type [26–28]. As noted, for example, in Ref. [23], usage of a

*FAX: +39-0382-987563. Silvano.Romano@pv.infn.it

lattice model produces significant savings in computational terms; moreover, it entails that a number a competing phases (e.g., smectic ones) are excluded from the start; notice that similar simplifications as for the possible phases are used in other named theoretical treatments as well.

Following and suitably modifying the line of reasoning in Ref. [9], we define and investigate here a minimal lattice model capable of producing (purely) tetrahedratic order.

In both cases the underlying idea is to construct the pair interaction via a simple geometric molecular model in terms of scalar products among two sets of unit vectors associated with the two interacting particles, respectively; the pair potential is written as a polynomial in the named scalar products; both the number of unit vectors and the polynomial order are given the smallest values consistent with the assumed molecular symmetry, and the sign of the interaction is chosen so as to produce an ordered ground state.

As for symbols and definitions, we are considering classical, identical particles, possessing T_d symmetry, whose centers of mass are associated with a three-dimensional (simple cubic) lattice $\mathbb{Z}^3$; let $\mathbf{x}_\mu \in \mathbb{Z}^3$ denote the coordinate vectors of their centers of mass; the interaction potential is taken to be isotropic in orientation space and restricted to nearest neighbors, involving particles or sites labeled by μ and ν, respectively. The orientation of each particle can be specified via an orthonormal triplet of three-component vectors (e.g., eigenvectors of its inertia tensor)—say, $\{\mathbf{w}_{\mu,\alpha},\ \alpha=1,2,3\}$; in turn, these are controlled by an ordered triplet of Euler angles $\omega_\mu=\{\phi_\mu,\theta_\mu,\psi_\mu\}$; particle orientations are defined with respect to a common, but otherwise arbitrary, Cartesian frame (which can, but need not, be identified with the lattice frame). It also proves convenient to use a simpler notation for the unit vectors defining orientations of two interacting molecules [29]—i.e., $\mathbf{u}_\alpha$ for $\mathbf{w}_{\mu,\alpha}$ and $\mathbf{v}_\gamma$ for $\mathbf{w}_{\nu,\gamma}$, respectively; here, for each α, $\mathbf{u}_\alpha$ and $\mathbf{v}_\alpha$ have the same functional dependences on ω_μ and ω_ν, respectively (pairs of corresponding unit vectors in the two interacting molecules); let $\tilde{\Omega}=\Omega_{\mu\nu}$ denote the set of Euler angles defining the rotation transforming $\mathbf{u}_\alpha$ into $\mathbf{v}_\alpha$; Euler angles will be defined here according to the convention used by Brink and Satchler, see also Ref. [30]. Moreover, let the orthonormal triplet of unit vectors associated with a lattice site be combined to yield four unit vectors $\{\mathbf{p}_{\mu,j},\ j=1,2,3,4\}$ arranged in a tetrahedral fashion—e.g.,

$$\begin{aligned}
\mathbf{p}_{\mu,1} &= c(+\mathbf{w}_{\mu,1}-\mathbf{w}_{\mu,2}-\mathbf{w}_{\mu,3}),\\
\mathbf{p}_{\mu,2} &= c(-\mathbf{w}_{\mu,1}+\mathbf{w}_{\mu,2}-\mathbf{w}_{\mu,3}),\\
\mathbf{p}_{\mu,3} &= c(-\mathbf{w}_{\mu,1}-\mathbf{w}_{\mu,2}+\mathbf{w}_{\mu,3}),\\
\mathbf{p}_{\mu,4} &= c(+\mathbf{w}_{\mu,1}+\mathbf{w}_{\mu,2}+\mathbf{w}_{\mu,3}),
\end{aligned} \tag{1}$$

where $c=\pm\sqrt{3}/3$ is an appropriate normalization factor.

It again proves convenient to use a simpler notation for the two sets of tetrahedral unit vectors in the two interacting molecules [29]—i.e., $\mathbf{e}_j$ for $\mathbf{p}_{\mu,j}$ and $\mathbf{f}_k$ for $\mathbf{p}_{\nu,k}$, respectively; let us finally define

$$h_{jk}=(\mathbf{e}_j\cdot\mathbf{f}_k). \tag{2}$$

An interaction potential consistent with the assumed symmetry can be written

$$\Psi=\Psi_{\mu\nu}=\sum_{j=1}^{4}\sum_{k=1}^{4}\mathcal{O}(h_{jk}), \tag{3}$$

where $\mathcal{O}(\cdots)$ denotes an odd function of its argument (notice that an even part alone would correspond to a higher, O_h, symmetry); $\mathcal{O}$ is also assumed to be analytical, so that Eq. (3) can be expanded as a convergent series of the form

$$\Psi=\sum_{l\geq 1}a_{2l+1}\left[\sum_{j=1}^{4}\sum_{k=1}^{4}h_{jk}^{2l+1}\right]=\sum_{l\geq 1}b_{2l+1}\left[\sum_{j=1}^{4}\sum_{k=1}^{4}P_{2l+1}(h_{jk})\right], \tag{4}$$

where $P_{2l+1}(\cdots)$ denotes Legendre polynomials of odd order; notice also that, by the underlying symmetry,

$$\sum_{j=1}^{4}\sum_{k=1}^{4}P_1(h_{jk})=\sum_{j=1}^{4}\sum_{k=1}^{4}P_2(h_{jk})=0. \tag{5}$$

The simplest interaction model expected to produce tetrahedratic order is obtained by setting a_3 or b_3 to negative quantities, and all other higher-order coefficients to zero; in other words,

$$\Psi=-\frac{9}{32}\epsilon\sum_{j=1}^{4}\sum_{k=1}^{4}h_{jk}^3=-\frac{9}{80}\epsilon\sum_{j=1}^{4}\sum_{k=1}^{4}P_3(h_{jk})=-\epsilon G_3(\tilde{\Omega}), \tag{6}$$

where ϵ denotes a positive quantity, setting energy and temperature scales (i.e., $T^*=k_BT/\epsilon$), and numerical factors have been adjusted by setting the minimum value to $-\epsilon$; let us define, also for future reference, the normalization factors

$$B_L=\frac{1}{4[P_L(1)+3P_L(-1/3)]},\quad L=3,4; \tag{7}$$

thus, $B_3=9/80$ and $B_4=27/112$, where B_3 actually appears in front of the second sum in Eq. (6).

Upon expanding $G_3(\tilde{\Omega})$ over the orthonormal basis of Wigner $\mathcal{D}$ functions [30] and comparing the resulting coefficients (the relevant integrals were calculated by means of MAPLE), it was found that its expression can be cast in the form

$$G_3(\tilde{\Omega})=\frac{1}{9}(+5S_{00}+\sqrt{10}S_{03}+2S_{33}), \tag{8}$$

where the three symbols S_{00}, S_{03}, and S_{33} denote symmetry-adapted combinations (see also Refs. [8,31,32]):

$$S_{00}=\mathcal{D}^3_{0,0}(\tilde{\Omega})=P_3(\cos\tilde{\theta})=(5\cos^3\tilde{\theta}-3\cos\tilde{\theta})/2, \tag{9}$$

$$\begin{aligned}
S_{03} &= \mathcal{D}^3_{0,3}(\tilde{\Omega})+\mathcal{D}^3_{3,0}(\tilde{\Omega})-\mathcal{D}^3_{-3,0}(\tilde{\Omega})-\mathcal{D}^3_{0,-3}(\tilde{\Omega})\\
&= (1/2)\sqrt{5}\sin^3\tilde{\theta}(\cos 3\tilde{\psi}-\cos 3\tilde{\phi}),
\end{aligned} \tag{10}$$

$$S_{33} = \mathcal{D}^3_{-3,-3}(\tilde{\Omega}) - \mathcal{D}^3_{+3,-3}(\tilde{\Omega}) - \mathcal{D}^3_{-3,+3}(\tilde{\Omega}) + \mathcal{D}^3_{+3,+3}(\tilde{\Omega})$$
$$= \frac{1}{4}[(1+\cos\tilde{\theta})^3 \cos 3(\tilde{\phi}+\tilde{\psi})$$
$$- (1-\cos\tilde{\theta})^3 \cos 3(\tilde{\phi}-\tilde{\psi})]. \quad (11)$$

II. MOLECULAR-FIELD TREATMENT AND SIMULATION METHODOLOGY

After applying a MF procedure [28], the resulting expression for the free energy has the form

$$A^*_{MF} = \rho s_3^2 - T^* \ln[\Xi/(8\pi^2)],$$

$$\Xi = \int_{Eul} \exp(\beta \tilde{W}) d\omega, \quad (12)$$

$$\tilde{W} = 2\rho s_3 G_3(\omega), \quad \beta = 1/T^*, \quad (13)$$

where $\int_{Eul}$ denotes integration over Euler angles; i.e., for any integrable function $\mathcal{F}(\omega)$,

$$\int_{Eul} \mathcal{F}(\omega) d\omega \equiv \int_0^{2\pi} d\phi \int_0^{\pi} \sin\theta \, d\theta \int_0^{2\pi} \mathcal{F}(\omega) d\psi; \quad (14)$$

here, $2\rho=6$ denotes the lattice coordination number and s_3 is the variational parameter (i.e., the order parameter). Moreover,

$$\frac{\partial A^*_{MF}}{\partial s_3} = 2\rho\tau,$$

$$\tau = s_3 - (1/\Xi) \int_{Eul} G_3(\omega) \exp(\beta \tilde{W}) d\omega; \quad (15)$$

the consistency equation $\tau=0$ can also be rewritten as

$$s_3 \Xi = \int_{Eul} G_3(\omega) \exp(\beta \tilde{W}) d\omega. \quad (16)$$

The free energy was minimized numerically for each temperature over a fine grid by means of numerical routines using both the function [Eq. (12)] and its derivative [Eq. (15)].

The obtained variational parameters can be then used to calculate the potential energy per particle U^*_{MF},

$$U^*_{MF} = \frac{\partial(\beta A^*_{MF})}{\partial\beta} = -\rho s_3^2, \quad (17)$$

where the consistency equation has been allowed for in the right-hand expression, and hence the configurational specific heat C^*_{MF}, by numerical differentiation; here and in following formulas, asterisks mean scaling by ϵ for energy quantities and scaling by k_B for the specific heat.

Results of the minimization procedure suggested that the parameter s_3 vanished continuously at the transition; therefore, we also considered Eq. (16) and used a power-series expansion with respect to s_3 for both integrals appearing in it; truncation at some low order n yielded a polynomial equation involving odd powers of s_3 only and whose coefficients were controlled by definite integrals of even powers of $G_3(\omega)$, up to exponent $(n+1)$, over the whole angular space. Notice that this procedure is usually applied to the nontrivial approximation of lowest order—i.e., $n=3$; here, as an additional comparison, the relevant integrals were calculated analytically, and the resulting polynomial equations of orders $n=3,5,7,9$ were solved in closed form by means of MAPLE. For each value of n, this procedure yielded only one solution continuously vanishing at $\Theta_{MF}=(6/7)\simeq 0.857143$, and in agreement with the results of the above numerical minimization procedure for T^* sufficiently close to Θ_{MF}; the usual asymptoptic behavior $s_3 \propto \sqrt{\Theta_{MF}-T^*}$ for $T^* \to \Theta_{MF}-0$ was found as well: in this case the value of proportionality coefficient was $(1/2)\sqrt{286}\simeq 8.4558$ and the asymptotic behavior was reached when $\Theta_{MF}-T^* \leq 10^{-6}$, whereas, for example, truncation at $n=5$ was adequate for $T^*=0.8571$.

A similar MF approach was worked out by Fel [10], but for a different interaction model; a Landau free energy density constructed in terms of scalar invariants of a third-rank ordering tensor was considered in Refs. [12,13], and both approaches yielded a second-order transition. On the other hand, available theoretical treatments point to the transition being driven first order by thermal fluctuations [10,12,13].

Simulations were carried out on a periodically repeated cubic sample, consisting of $V=q^3$ particles, $q=10,12,16,20,24,32$; calculations were run in cascade, in order of increasing temperature; each cycle (or sweep) consisted of $2V$ Monte Carlo (MC) steps, including a sublattice sweep [33]; the finest temperature step used was $\Delta T^*=0.0005$ in the transition region (but see also below for additional simulations). Different random-number generators were used, as discussed in Ref. [33].

Equilibration runs took between 25 000 and 100 000 cycles, and production runs took between 250 000 and 1 000 000; macrostep averages for evaluating statistical errors were taken over 1000 cycles. Calculated thermodynamic quantities include mean potential energy per site, U^*, and configurational specific heat per particle, C^*.

Since interactions of tetrahedral symmetry are expected to produce secondary cubatic correlations as well, we worked out structural quantities of both types. As for the frame-independent (rotationally invariant) order parameters, let

$$M_L = \sqrt{B_L \sum_{\lambda=1}^{V} \sum_{\nu=1}^{V} [\sum_{j=1}^{4} \sum_{k=1}^{4} P_L(\mathbf{p}_{\lambda,j} \cdot \mathbf{p}_{\nu,k})]}, \quad L=3,4; \quad (18)$$

then, the simulation estimate for the order parameters is

$$s_L = \frac{1}{V}\langle M_L \rangle \quad (19)$$

and the associated susceptibilities read

$$\chi_L = \frac{1}{V}\beta(\langle M_L^2 \rangle - \langle M_L \rangle^2). \quad (20)$$

Notice also that, by the addition theorem for spherical harmonics [30], the double sums appearing in Eq. (18) actually reduce [8,9] to linear combinations of the squares of the simpler quantities

$$\xi_{j,L,m} = \sum_{\mu=1}^{V} \mathrm{Re}[C_{L,m}(\mathbf{p}_{\mu,j})],$$

$$\eta_{j,L,m} = \sum_{\mu=1}^{V} \mathrm{Im}[C_{L,m}(\mathbf{p}_{\mu,j})]; \tag{21}$$

here, $m=0,1,\ldots,L$ and $C_{L,m}(\cdots)$ are modified spherical harmonics, and Re and Im denote real and imaginary parts, respectively; in turn, each spherical harmonics is a suitable polynomial constructed in terms of Cartesian components of the corresponding unit vector (see, e.g., Ref. [34]); in this case first- and second-rank order parameters are zero by symmetry [28].

One can also evaluate the so-called short-range order parameter [35,36]

$$\sigma_L = B_L \left\langle \sum_{j=1}^{4} \sum_{k=1}^{4} P_L(h_{jk}) \right\rangle, \quad L=3,4, \tag{22}$$

measuring correlations between pairs molecules associated with nearest-neighboring sites; in the present case, the functional form of the interaction potential entails that the potential energy is proportional to σ_3—i.e., $U^*=-\rho\sigma_3$. Moreover, long- and short-range orientational order can be compared via the correlation excesses

$$r_L = \sigma_L - s_L^2. \tag{23}$$

III. RESULTS AND COMPARISONS

As mentioned above, the MF treatment predicted a second-order transition; thus, the order parameter decreased continuously and monotonically, vanishing at $\Theta_{MF}=6/7$, where the specfic heat exhibited a discontinuous jump to zero; its limit as $T^* \to \Theta_{MF}-0$ was found to be 429/2; on the other hand, simulation results (Figs. 1–9) pointed to a different scenario.

Simulation results for the short-range order parameters σ_3 (and hence the potential energy U^*) and σ_4, Figs. 1 and 2, respectively, were found to be independent of sample size for $T \lesssim 0.68$ and then $T \gtrsim 0.72$, and showed a pronounced sample-size dependence in between; actually, for $q=24$, the two figures exhibited a pronounced jump taking place over a temperature range of 0.0005 between the two values $T_2^*=0.6895$ and $T_3^*=0.690$; for $q=32$, the jump appeared to take place between $T_1^*=0.689$ and T_2^*. Figures 4 and 5 showed a similar pattern as for the jumps of the long-range order parameters s_L, taking place at the same temperature as for U^*; on the other hand, in the low-temperature régime, sample-size effects appeared to become rather mild for $q \gtrsim 20$, whereas the high-temperature region exhibited a pronounced decrease of s_L with increasing sample size.

Both configurational specific heat (Fig. 3) and susceptibilities (Figs. 6 and 7) peaked around the same temperature,

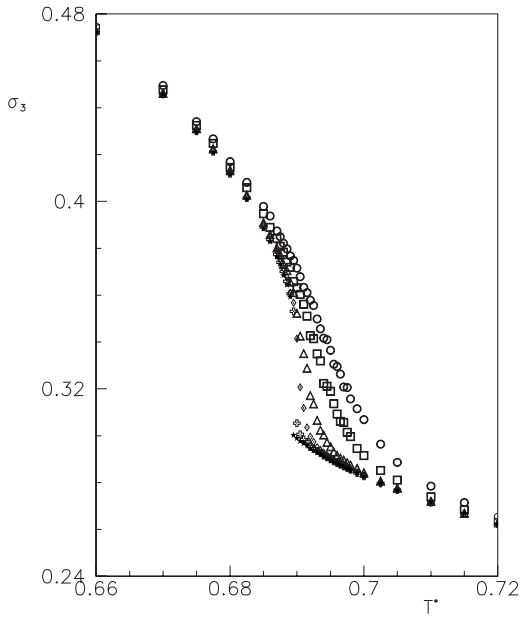

FIG. 1. Simulation results for the short-range order parameter σ_3, obtained with different sample sizes. Circles, $q=10$; squares, $q=12$; triangles, $q=16$; lozenges, $q=20$; crosses, $q=24$; stars, $q=32$. Unless otherwise stated or shown, here and in the following figures, the associated statistical errors fall within symbol sizes. See also the text about additional simulations carried out in the transition region.

corresponding to the above jumps; they showed a recognizable sample-size dependence over the named temperature range $0.68 \lesssim T^* \lesssim 0.72$ and were again largely unaffected by sample sizes outside it.

Simulation results for the correlation excess are plotted in Figs. 8 and 9, where the transition is signaled by a recognizable jump; in the disordered region, sample-size effects ap-

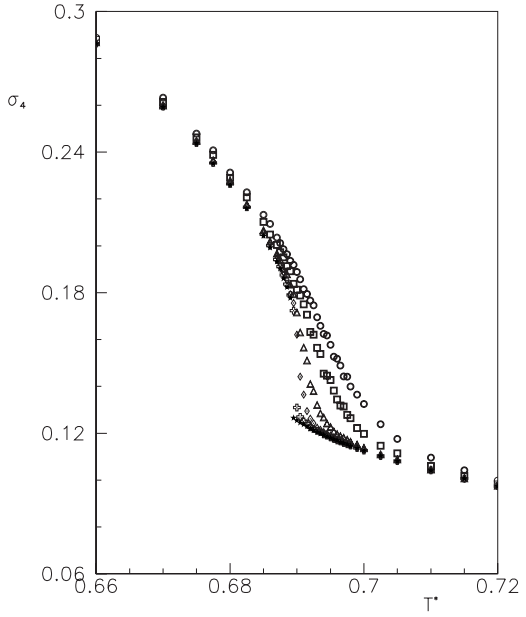

FIG. 2. Simulation results for the short-range order parameter σ_4; same meaning of symbols as in Fig. 1.

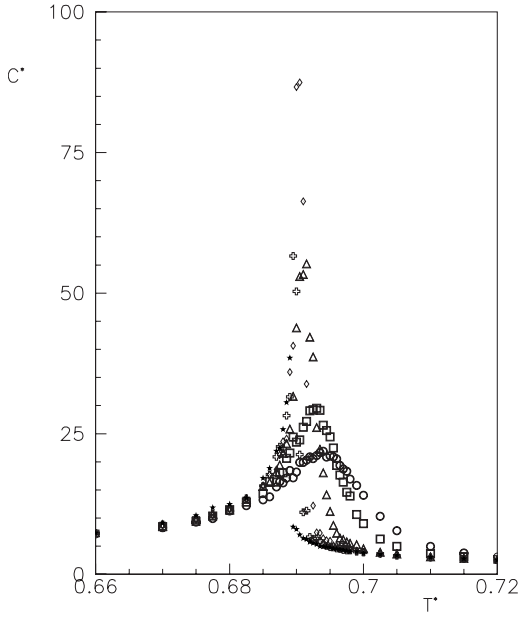

FIG. 3. Simulation results for the configurational heat capacity; same meaning of symbols as in Fig. 1; here, as well as in the following Figs. 6 and 7, the associated statistical errors, not shown, range between 1% and 5%.

pear to saturate for $q \geq 20$; notice also that r_3 peaks at transition, whereas r_4 (a "secondary" quantity) keeps decreasing with increasing temperature.

Thus we propose a first-order transition and the value $\Theta_{MC}=0.690 \pm 0.001$, for the transition temperature; here, the error bar is conservatively taken to be twice the temperature step used in the transition region. Upon analyzing the simulation results for the largest sample at the two temperatures

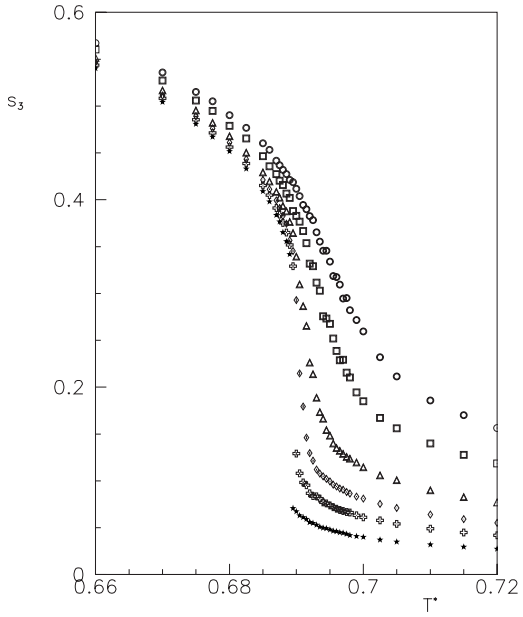

FIG. 4. Simulation results for the long-range order parameter s_3, obtained with different sample sizes; same meaning of symbols as in Fig. 1.

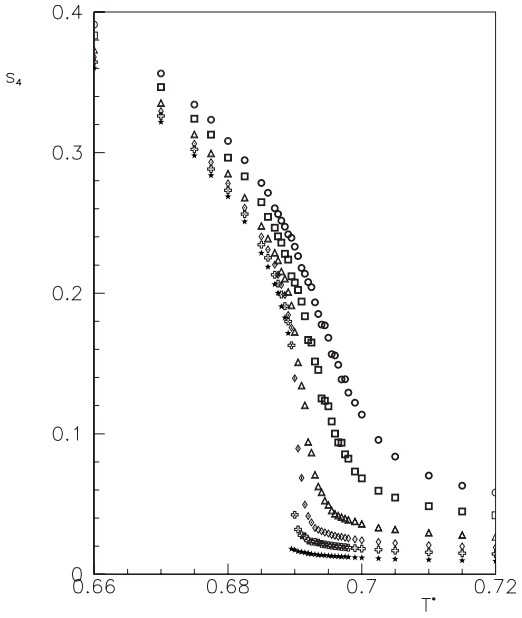

FIG. 5. Simulation results for the long-range order parameter s_4, obtained with different sample sizes; same meaning of symbols as in Fig. 1.

T_1^* and T_2^* as discussed in Refs. [37,38], we obtained the following estimates for transitional properties:

$$s_3 = 0.342 \pm 0.015, \quad s_4 = 0.172 \pm 0.015,$$

$$\Delta\sigma_3 = -0.06 \pm 0.01, \quad \Delta\sigma_4 = -0.052 \pm 0.007,$$

$$\Theta_{MC} = 0.690 \pm 0.001, \quad \Delta U^* = 0.18 \pm 0.03,$$

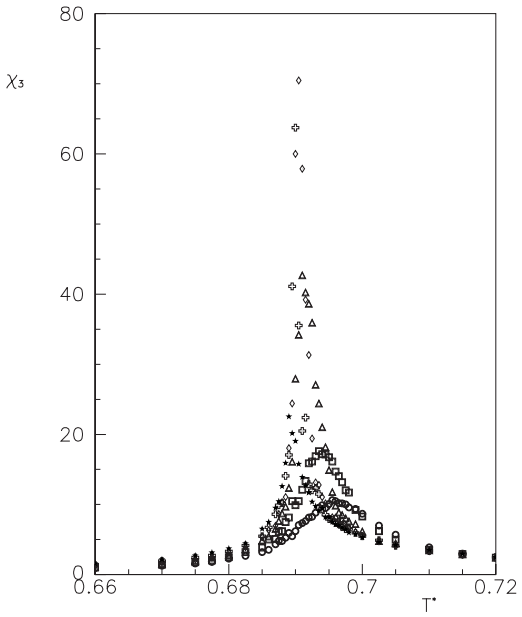

FIG. 6. Simulation results for the order parameter susceptibility χ_3, obtained with different sample sizes: same meaning of symbols as in Fig. 1.

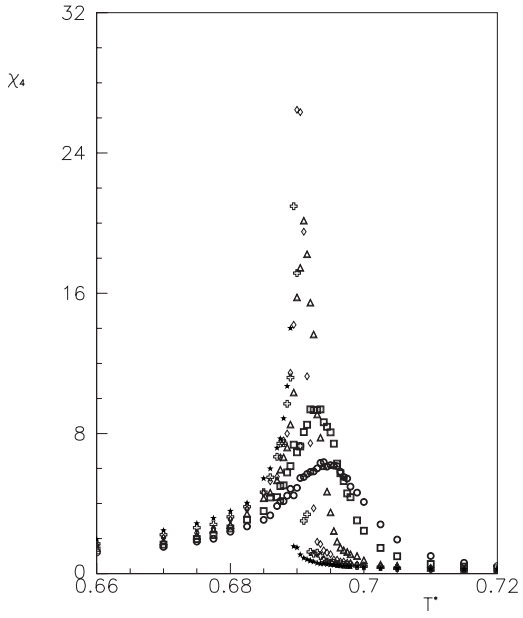

FIG. 7. Simulation results for the order parameter susceptibility χ_4, obtained with different sample sizes: same meaning of symbols as in Fig. 1.

Actually, the same analysis was also applied to simulation results obtained for $q=24$ and the two temperatures T_2^* and T_3^*, and yielded results consistent with the ones listed here; let us mention, for comparison, that the ratio Θ_{MC}/Θ_{MF} is $\simeq 0.805$ versus $\simeq 0.878$ for the cubatic model discussed in Ref. [9] and $\simeq 0.856$ [22] for the model proposed by Lebwohl and Lasher (LL) and used for their seminal simulation papers in the early 1070s [24,25]; in the two latter cases both MF and MC models yield a first-order transition.

To the temperature step used ($\Delta T=0.0005$), the maxima of specific heat and susceptibility did not appear to increase

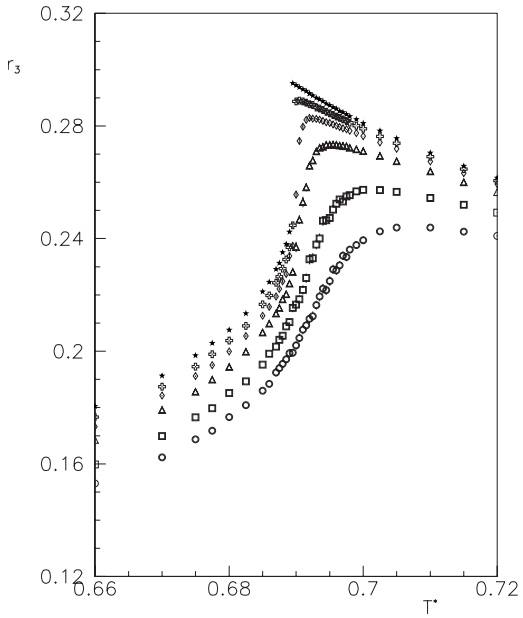

FIG. 8. Simulation results for the correlation excess r_3 [see Eq. (23)], obtained with different sample sizes: same meaning of symbols as in Fig. 1.

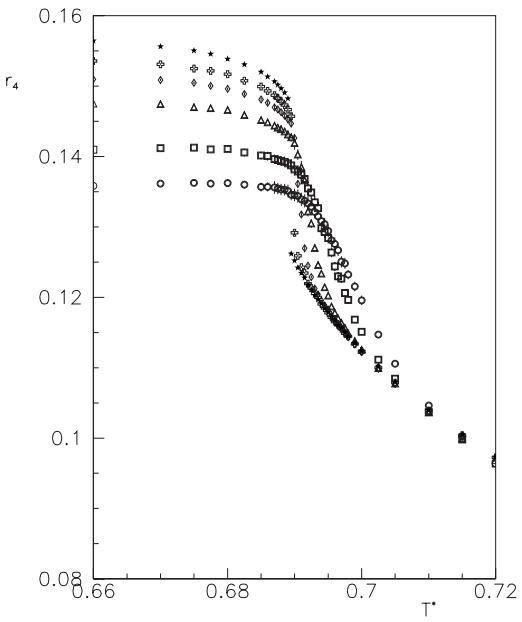

FIG. 9. Simulation results for the correlation excess r_4 [see Eq. (23)], obtained with different sample sizes: same meaning of symbols as in Fig. 1.

monotonically with q; this suggests that, for larger samples, the "real" maxima may be attained somewhere else in the transition region. Additional and longer simulations (up to 2 000 000 cycles) were therefore run for $q>12$ around the temperatures where the specific heat attains its maximum and using a finer temperature step $\Delta T=0.0001$. For $q=16$, the simulation results for specific heat and susceptibility remained roughly constant within associated statistical errors between $T_3^*=0.6905$ and $T_4^*=0.6915$, and the maxima did not increase; on the other hand, for $q=20,24,32$, the maxima so determined did show a recognizable increase with q (these new results were not added to the figures for reasons of readability). Let now $\tilde{T}^*(q)$ denote for each q, the temperature where the specific heat C^* attains its maximum $\tilde{C}^*(q)$; the values so determined were $\tilde{T}^*(10)=0.694$, $\tilde{T}^*(12)=0.693$, $\tilde{T}^*(16)=0.6915$, $\tilde{T}^*(20)=0.6904$, $\tilde{T}^*(24)=0.6898$, and $\tilde{T}^*(32)=0.6892$; for example, when $q=32$, $\tilde{C}^*(32)=457\pm 9$; plots of $\ln \tilde{C}^*(q)$ versus $\ln q$ (not reported) showed a linear dependence as well as a slope close to 3 for $q>12$. Histograms for the above macrostep averages of potential energy and order parameter at the temperatures $\tilde{T}^*(q)$ were also produced; the histograms developed a recognizable two-peak structure when $q>16$; moreover, for $q>20$, the abscissas of the two peaks were in broad agreement with the estimates of the corresponding transitional properties as listed above.

To summarize, we have defined a minimal tetrahedratic mesogenic lattice model (so to speak, the tetrahedratic counterpart of the LL model), involving continuous interactions, and investigated it by MF and MC models; the MF model predicts a second-order transition to an isotropic phase, and other available theoretical treatments point to the transition being driven first order by thermal fluctuations. Simulations showed evidence of a first-order transition.

As for the place of the present paper within current liquid crystal research, on the one hand, our simulation results substantiate other theoretical treatments as mentioned in the Introduction, moving beyond the MF or Landau approximations under which they were obtained; on the other hand, this is a minimal lattice model (see also remarks in the Introduction), but still capable of producing the required salient feature, whereas other theoretical treatments allow for first-, second-, and third-rank interactions [13], producing richer phase sequences. In the future one can envisage a number of extensions or consider other somehow related models: for example one can think of a pure excluded-volume (hard-core) interaction model; this approach has been used for uniaxial, biaxial, and cubatic counterparts (see also the Introduction), but, as far as we could check, not for tetrahedratic phases. Still giving up the lattice, one can think of soft-core models where positional coordinates are continuous variables, the orientational interaction is modulated by some function of the distance R between centers of mass, and a purely positional term (another appropriate function of R) is taken into account, so as to produce liquid cohesion; in the case of uniaxial mesogenic models, this approach can be traced back to Ref. [39]. Let us finally mention that rigid tetrahedra have been considered here, whereas other theoretical treatments allow for their deformability by external fields or flows [40].

ACKNOWLEDGMENTS

The present extensive calculations were carried out on, among other machines, workstations belonging to the Sezione di Pavia of Istituto Nazionale di Fisica Nucleare (INFN); allocations of computer time by the Computer Centre of Pavia University and CILEA (Consorzio Interuniversitario Lombardo per l' Elaborazione Automatica, Segrate, Milan), as well as by CINECA (Centro Interuniversitario Nord-Est di Calcolo Automatico, Casalecchio di Reno, Bologna), are gratefully acknowledged. The author also wishes to thank Professor E. G. Virga (Pavia, Italy), Professor H. Pleiner (Max Planck Institute for Polymer Research, Mainz, Germany), Dr. L. G. Fel (Technion, Haifa, Israel), and Dr. R. Blaak (Cambridge University, Cambridge, England) for helpful discussions and suggestions. Finally, the author gratefully acknowledges financial support from the Italian Ministry for Higher Education (MIUR) through PRIN Grant No. 2004024508.

[1] B. R. Acharya, A. Primak, and S. Kumar, Liq. Cryst. Today **13**(1), 1 (2004).
[2] L. A. Madsen, T. J. Dingemans, M. Nakata, and E. T. Samulski, Phys. Rev. Lett. **92**, 145505 (2004).
[3] B. R. Acharya, A. Primak, and S. Kumar, Phys. Rev. Lett. **92**, 145506 (2004).
[4] J.-H. Lee, T.-K. Lim, W.-T. Kim, and J.-I. Jin, J. Appl. Phys. **101**, 034105 (2007).
[5] G. R. Luckhurst, Angew. Chem. Int. Ed. Engl. **44**, 2834 (2005).
[6] G. De Matteis, S. Romano, and E. G. Virga, Phys. Rev. E **72**, 041706 (2005).
[7] M. V. Jarić, Nucl. Phys. B **265**, 647 (1986).
[8] R. Blaak and B. M. Mulder, Phys. Rev. E **58**, 5873 (1998).
[9] S. Romano, Phys. Rev. E **74**, 011704 (2006).
[10] L. G. Fel, Phys. Rev. E **52**, 702 (1995).
[11] L. G. Fel, Phys. Rev. E **52**, 2692 (1995).
[12] L. Radzihovsky and T. C. Lubensky, Europhys. Lett. **54**, 206 (2001).
[13] T. C. Lubensky and L. Radzihovsky, Phys. Rev. E **66**, 031704 (2002).
[14] P. E. Cladis, H. R. Brand, and H. Pleiner, Liq. Cryst. Today **9**(3–4), 1 (1999).
[15] H. R. Brand, P. E. Cladis, and H. Pleiner, Europhys. Lett. **57**, 368 (2002).
[16] H. R. Brand, P. E. Cladis, and H. Pleiner, Ferroelectrics **315**, 165 (2005).
[17] B. Mettout, Phys. Rev. E **74**, 041701 (2006).
[18] G. Pelzl, S. Diele, and W. Weissflog, Adv. Mater. **11**, 707 (1999).
[19] J. Matraszek, J. Mieczkowski, J. Szydłowska, and E. Gorecka, Liq. Cryst. **27**, 429 (2000).
[20] P. J. Camp, M. P. Allen, and A. J. Masters, J. Chem. Phys. **111**, 9871 (1999).
[21] J. Peláez and M. R. Wilson, Phys. Rev. Lett. **97**, 267801 (2006).
[22] P. Pasini, C. Chiccoli, and C. Zannoni, in *Advances in the Computer Simulations of Liquid Crystals*, edited by P. Pasini and C. Zannoni, NATO Science Series, Vol. C545 (Kluwer, Dordrecht, 2000), Chap. 5.
[23] M. A. Bates and G. R. Luckhurst, Phys. Rev. E **72**, 051702 (2005).
[24] G. Lasher, Phys. Rev. A **5**, 1350 (1972).
[25] P. A. Lebwohl and G. Lasher, Phys. Rev. A **6**, 426 (1972).
[26] W. Maier and A. Saupe, Z. Naturforsch. A **13**, 564 (1958); W. Maier and A. Saupe, *ibid.* **14**, 882 (1959); W. Maier and A. Saupe, *ibid.* **15**, 287 (1960).
[27] G. R. Luckhurst, in *The Molecular Physics of Liquid Crystals*, edited by G. R. Luckhurst and G. W. Gray (Academic Press, London, 1979), Chap. 4, pp. 85–120.
[28] G. R. Luckhurst, in *Physical Properties of Liquid Crystals: Nematics*, edited by D. A. Dunmur, A. Fukuda, and G. R. Luckhurst (INSPEC, London, 2001), Chap. 2.1.
[29] C. Chiccoli, P. Pasini, F. Semeria, and C. Zannoni, Int. J. Mod. Phys. C **10**, 469 (1999).
[30] D. A. Varshalovich, A. N. Moskalev, and V. K. Khersonskii, *Quantum Theory of Angular Momentum* (World Scientific, Singapore, 1988).
[31] B. M. Mulder, **1**, 539 (1986).
[32] B. Mulder, Phys. Rev. A **39**, 360 (1989).
[33] R. Hashim and S. Romano, Int. J. Mod. Phys. B **13**, 3879 (1999).
[34] J. W. Leech and D. J. Newman, *How to Use Groups* (Methuen, London, 1969).

[35] C. Zannoni, in *The Molecular Physics of Liquid Crystals*, edited by G. R. Luckhurst and G. W. Gray (Academic Press, London, 1979), Chaps. 3 and 9.
[36] C. Zannoni, in *Advances in the Computer Simulations of Liquid Crystals*, edited by P. Pasini and C. Zannoni, NATO Science Series, Vol. C545 (Kluwer, Dordrecht, 2000), Chap. 2.
[37] S. Romano, Int. J. Mod. Phys. B **16**, 2901 (2002).
[38] S. Romano, Physica A **324**, 606 (2003).
[39] G. R. Luckhurst and S. Romano, **373**, 111 (1980).
[40] P. E. Cladis, H. Pleiner, and H. R. Brand, Eur. Phys. J. E **11**, 283 (2003).